Earthline Journal of Chemical Sciences
E-ISSN: 2581-9003; CODEN: EJCSB4
Volume 9, Number 2, 2023, Pages 163-176
https://doi.org/10.34198/ejcs.9223.163176

Interaction of DMAZ and TEMED - A DFT Treatise

Lemi Türker

Department of Chemistry, Middle East Technical University, Üniversiteler, Eskişehir Yolu No: 1, 06800 Çankaya/Ankara, Turkey; e-mail: lturker@gmail.com; lturker@metu.edu.tr

Abstract

In the present study, interaction of DMAZ and TEMED has been investigated within the limitations of density functional theory at the level of B3LYP/6-31++G(d,p). DMAZ is an explosive material but it is also oxidant constituent of some hypergolic systems. TEMED or TEMEDA acts as the partner of DMAZ. The interaction has been investigated and the findings reveal that in the absence of any hypergolic reaction, the interaction is of mainly electrostatic in nature, no bond cleavages or new bond formations happen. The variations are only of conformational in character. The composite is electronically stable in the static conditions and thermally favorable. Some quantum chemical, electronic and spectral data have been collected and discussed.

1. Introduction

The term hypergolicity is meant spontaneous ignition of a fuel and an oxidizer which is in contact. Hypergolic propellants are preferred mostly for several rocket propulsion missions, when multiple and reliable ignitions are required for mission success [1-4]. The conventional hypergolic system is composed of hydrazine as the fuel component, which is a very toxic chemical. Hawkins *et al.* taught a bipropellant fuel based upon salts containing the dicyanamide anion, employing nitrogen-containing, heterocyclic-based cations such as the imidazolium cation [5]. While salt molecules contain highly energetic (formation of enthalpy), high nitrogen anions, the dicyanamide-based molecule solely displays fast ignition. Hypergolic liquid or gel fuel mixtures utilized in bipropellant propulsion systems are used instead of fuels containing toxic monomethylhydrazine. Usually, the fuel mixtures of hypergolic systems include one or more amine azides mixed with one or more tertiary diamine, tri-amine or tetra-amine compounds. Mostly, the fuel

Received: September 29, 2022; Accepted: November 5, 2022; Published: November 11, 2022

Keywords and phrases: DMAZ; TEMED; TMEDA; hypergolic; explosives; DFT.

mixtures include TMEDA (TEMED, N,N,N',N'-tetramethylethylenediamine) mixed with DMAZ (2-N,N-dimethylaminoethylazide) or TMEDA mixed with TAEA, (tris(2-azidoethyl)amine) and TMEDA mixed with one or more cyclic amine azides. In principle, each hypergolic fuel mixture manages to reduce the ignition delay when the components come in contact with each other (fuel and oxidant) in propellant systems [3]. Various patents and articles exist in the literature about hypergolic mixtures [4-20]. A conventional, storable bipropulsion system uses hydrazine or a hydrazine derivative (e.g., monomethylhydrazine) as the fuel component. A typical fuel affords useful performance characteristics and possesses a fast ignition with the oxidizer. This fast (hypergolic) ignition provides system reliability for on-demand action of the propulsion system. However, the conventional, storable bipropulsion system is limited by its inherent energy density that can be traced, in large measure, to the density of the fuel. In some hypergolic systems, there are significant costs and operational constraints associated with handling the fuel that derives from the fuel's very toxic vapor. Some alternative hypergolic mixtures have been investigated which are less toxic or environmentally friendly [8,13,14]. On the other hand, mechanism of explosion induced by contact of hypergolic liquids has attracted attention for many years [19,20]. Note that the chemical processes governing the ignition of reacting flows comprise many reactions between a fuel, an oxidizer, intermediate species, and products. Those are also governed by an interaction between heat release rate and heat loss rate. In the present treatise, DMAZ and TEMED which constitute a hypergolic mixture are considered in vacuum conditions. The present study aims to get a static picture of the DMAZ and TEMED interaction (in the absence of any hypergolic reaction) within the limitations of the density functional theory (DFT) and the basis set employed.

2. Method of Calculation

In the present study, all the initial geometry optimizations of the structures leading to energy minima were achieved by using MM2 method then followed by semi-empirical PM3 self-consistent fields molecular orbital (SCF MO) method [21,22] at the unrestricted level [23]. Afterwards, the structure optimizations have been managed within the framework of Hartree-Fock (HF) and finally by using density functional theory (DFT) at the level of B3LYP/6-31++G(d,p) [24,25]. Note that the exchange term of B3LYP consists of hybrid Hartree-Fock and local spin density (LSD) exchange functions with Becke's gradient correlation to LSD exchange [26]. Also note that the correlation term of B3LYP consists of the Vosko, Wilk, Nusair (VWN3) local correlation functional [27]

and Lee, Yang, Parr (LYP) correlation correction functional [28]. Presently, a rather high level of basis set has been employed in order to minimize the basis set superposition error [23,29]. In the present study, the normal mode analysis for each structure yielded no imaginary frequencies for the 3*N*–6 vibrational degrees of freedom, where *N* is the number of atoms in the system. This indicates that the structure of each molecule corresponds to at least a local minimum on the potential energy surface. Furthermore, all the bond lengths were thoroughly searched in order to find out whether any bond cleavage occurred or not during the geometry optimization process. All these computations were performed by using SPARTAN 06 [30].

3. Results and Discussion

TEMED, (N,N,N',N'-Tetramethyl ethylenediamine $(CH_3)_2NCH_2CH_2N(CH_3)_2$) (Synonyms: TMEDA, 1,2-Bis(dimethylamino)ethane) and DMAZ (2-dimethyl-aminoethylazide, 2-Azido-N,N-dimethylethan-1-amine or dimethyl(2-azidoethyl)amine)) TEMED can be a component of hypergolic propellants. DMAZ has been introduced as a non-carcinogenic fuel with high performance as compared to the best available fuels. The results showed that DMAZ is not sensitive to impact, direct flame and shock wave. Meanwhile, it has moderate and high sensitivity to electrostatic discharge and heat in confined volume, respectively [31].

In hypergolic explosives DMAX acts as an oxidizing agent but it is an explosive as well. Explosives have some sorts of redox potential. They act either as intramolecular redox agent, in which some parts/groups of the molecule acts as an oxidizer agent, and some parts/groups of the same molecule behave as a reducing agent. On the other hand, in the case of intermolecular explosives, an oxidizer and a reducer parts/groups are on different molecules [32].

Figure 1 shows the optimized structures as well as the direction of the dipole moment vectors of the systems considered presently. Note the nonlinear structure of the azide group in DMAX. The dipole moment vectors are 3.15, 1.06 and 2.95 debye for DMAZ, TEMED and their 1:1 composite, respectively. As for the polarizability values, they are 50.25, 52.45 and 62.59 10^{-30} m^3 units, respectively for DMAZ, TEMED and DMAZ+ TEMED. The H^o and G^o values of the composite are -1902937.198 and -1903098.796 kJ/mol., respectively whereas S^o is 542.01 J/mol^o.

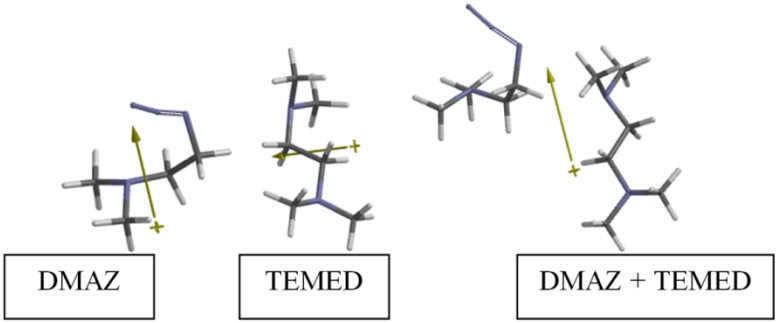

Figure 1. Optimized structures of the systems considered.

Figure 2 shows the calculated IR spectra of the systems considered. In the spectrum of DMAZ various symmetrical and antisymmetrical C-H vibrations occur in the region of 3126-2932 cm^{-1}. The sharp peak at 2246 cm^{-1} stands for the azide group. The C-H vibrations of TEMED occur at 3130-2910 cm^{-1}. In the case of the composite, various symmetrical and antisymmetrical C-H vibrations happen in the region of 3129-2908 cm^{-1}. The sharp peak at 2241 cm^{-1} stands for the vibrations of the azide moiety. As the data reveal, some small shifts occur in the frequencies of the composite when they are compared with the respective data of the components.

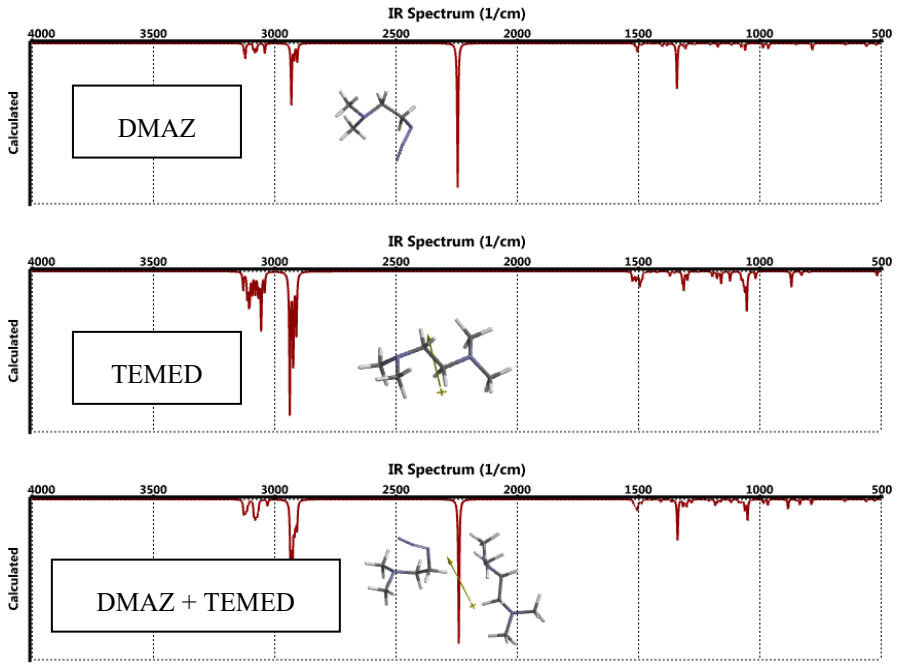

Figure 2. The calculated IR spectra of the systems considered.

Figure 3 shows the electrostatic potential charges (ESP) on the atoms of the systems considered. Note that the ESP charges are obtained by the program based on a numerical method that generates charges that reproduce the electrostatic potential field from the entire wavefunction [30].

Compared to charges on the respective positions of the components and the composite, some variations are observed, especially in the charges of the carbon atoms and the nitrogens of TEMED.

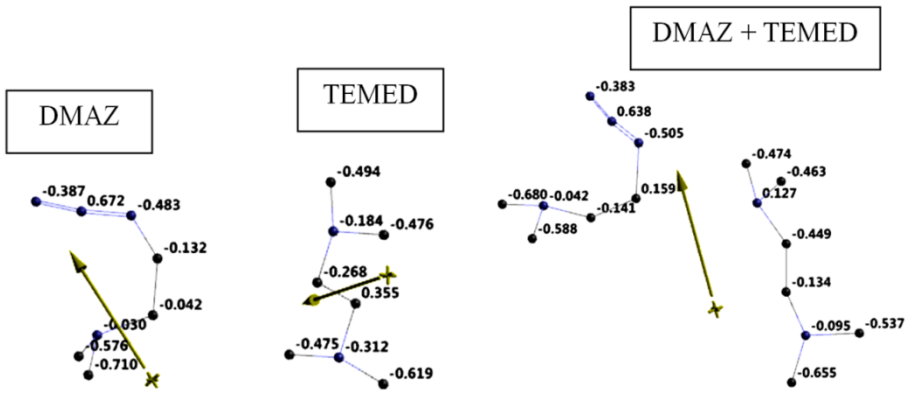

Figure 3. ESP charges on the atoms of the components and the composite (hydrogens not shown).

Figure 4 displays the ESP maps of the components and the composite. As seen in the figure, negative charge population resides on the terminal nitrogen of the azide group and the presence of DMAZ somewhat affects TEMED. Figure 5 shows potential maps of the components and the composite. Both of the figures reflect the interaction between the components.

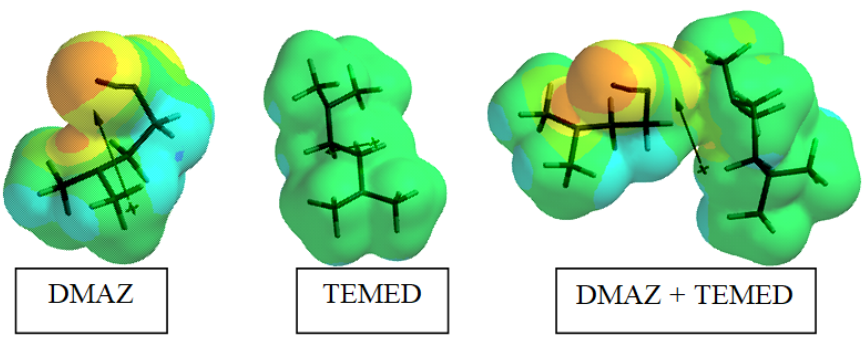

Figure 4. ESP maps of the components and the composite.

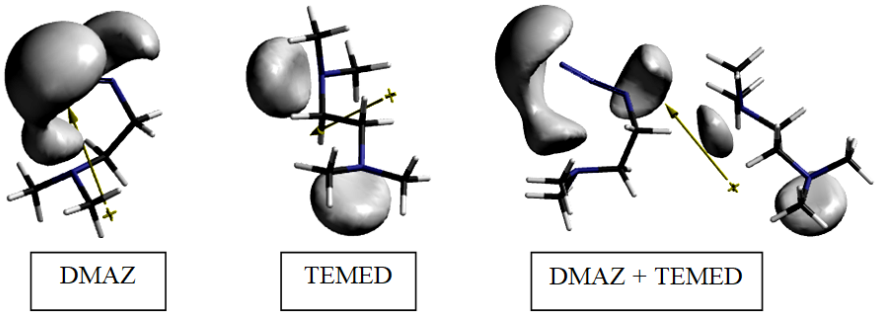

Figure 5. Potential maps of the components and the composite.

Figure 6 displays some of the molecular orbital energy levels of the systems considered.

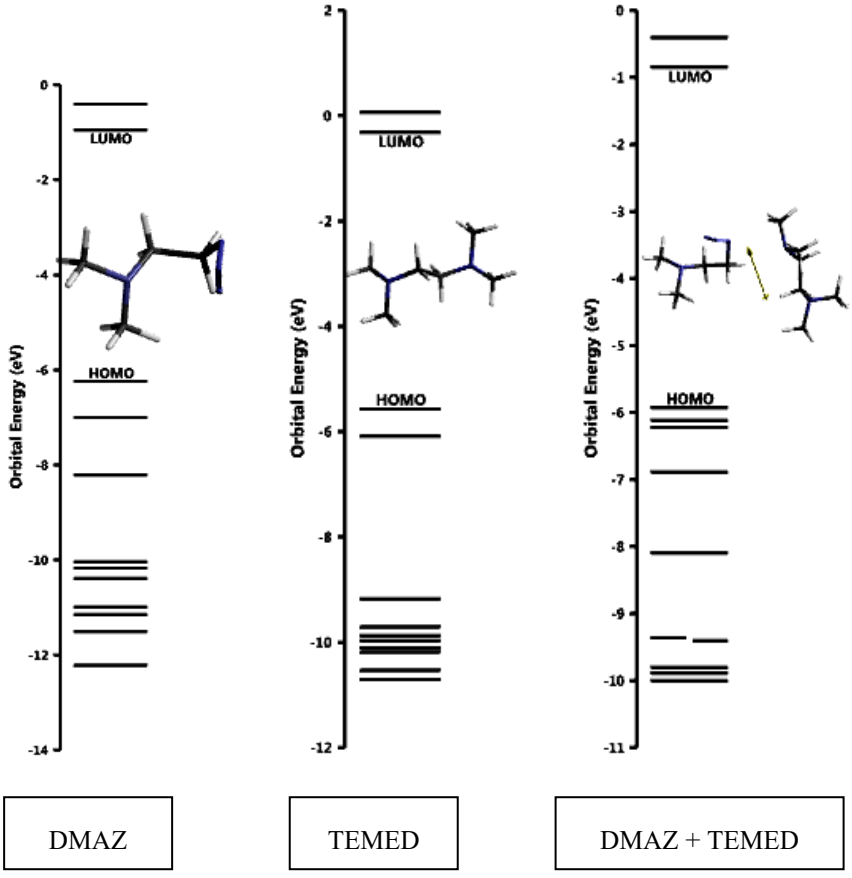

Figure 6. Some of the molecular orbital energy levels of the systems.

The frontier molecular orbital energy levels (ε_{HOMO} and ε_{LUMO}) and the interfrontier molecular orbital energy gap values ($\Delta\varepsilon$, $\Delta\varepsilon=\varepsilon_{LUMO}-\varepsilon_{HOMO}$) are listed in Table 1. The orders of HOMO and LUMO energies are the same and it is DMAZ < TEMED + DMAZ < TEMED. The order of $\Delta\varepsilon$ values is TEMED + DMAZ < TEMED < DMAZ.

Table 1. The HOMO, LUMO energies and $\Delta\varepsilon$ values of the systems considered.

	HOMO	LUMO	$\Delta\varepsilon$
TEMED	-537.15	-30.44	506.71
DMAZ	-602.15	-91.95	510.20
TEMED + DMAZ	-572.35	-81.99	490.36

Energies in kJ/mol.

The frontier molecular orbital energy levels of the composite is in between the respective values of the components. So, the way of interaction between the components shows (as expected) that TEMED supplies some electron population to DMAZ, raising up the HOMO and LUMO energy levels of DMAZ, while the HOMO and LUMO energy levels of TEMED are lowered by the influence of DMAZ. On the other hand, the azide group should have lowered both the HOMO and LUMO energy levels of DMAZ, due to inductive and electronic effects. It should be more effective than energy raising effect of dimethyl amino group attached to the other end of DMAZ molecule. As for the other component, TEMED, it has two of the dimethylamino groups at the opposite terminals of ethyl moiety and it has the HOMO and LUMO energies highest of all the systems. Consequently the $\Delta\varepsilon$ values follow the order of TEMED + DMAZ < TEMED < DMAZ. Note that none of the components and the complex has an extended conjugation (the azide group possesses orthogonal π-skeleton). This fact is reflected in the UV-VIS spectra of the systems (Figure 7) which look alike and confined to UV region.

Figure 7 shows The calculated UV-VIS spectra (time dependent DFT) of the systems considered.

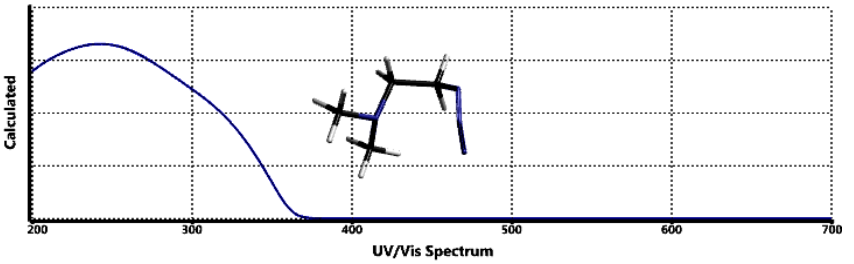

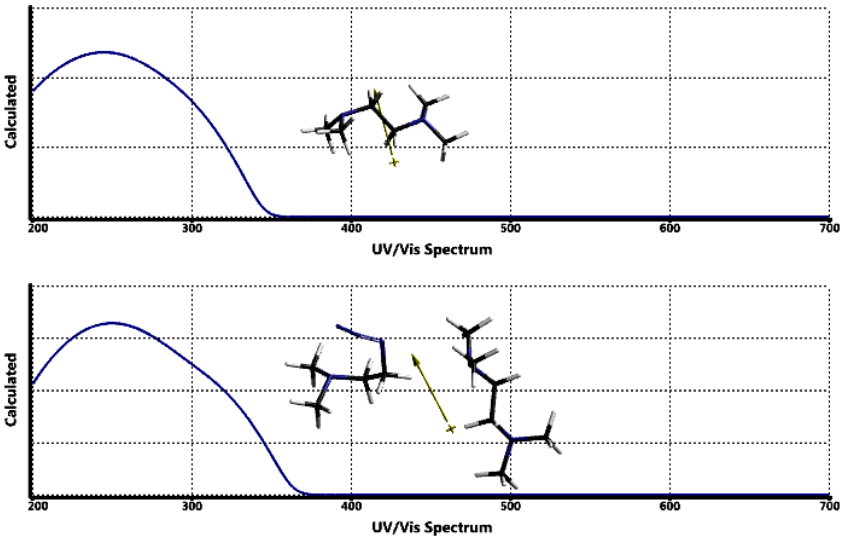

Figure 7. The calculated UV-VIS spectra of the systems considered.

Table 2 lists the λ_{max} values of the systems considered. As seen in the table, the order of λ_{max} values is DMAZ < TEMED + DMAZ < TEMED which is not the same as the order of $\Delta\varepsilon$ values. It implies that in dictating the λ_{max} values, some other factors rather than simply the HOMO-LUMO transition ($\Delta\varepsilon$) is effective but some other factors e.g., the transition moment plays [33,34] a role (or both).

Table 2. λ_{max} values of the systems considered.

	DMAZ	TEMED	DMAZ+ TEMED
λ_{max}	244.08	250.62	246.86

λ_{max} values in nm.

Figure 8 displays the HOMO and LUMO patterns of the systems considered. As seen there, in the composite the HOMO mainly spreads over TEMED component and the LUMO is on DMAZ only. Whereas in the case of HOMO-1 (NEXT HOMO) and LUMO+1 (NEXT LUMO) orbitals the main contributions to the composite come from DMAZ (see Figure 9).

Figure 10 shows the bond density of the composite in which the electron population concentrates over the components but there exists none in the region between the components.

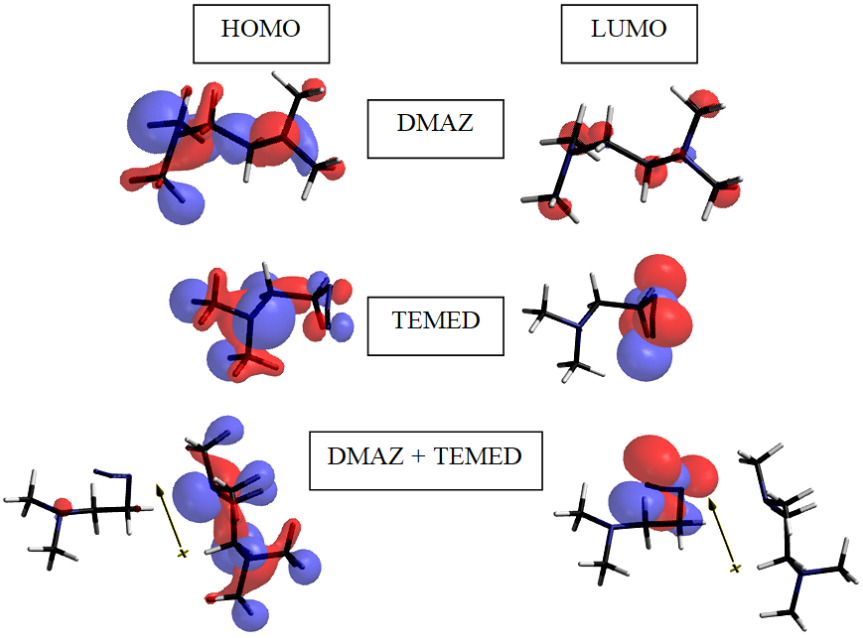

Figure 8. The HOMO and LUMO patterns.

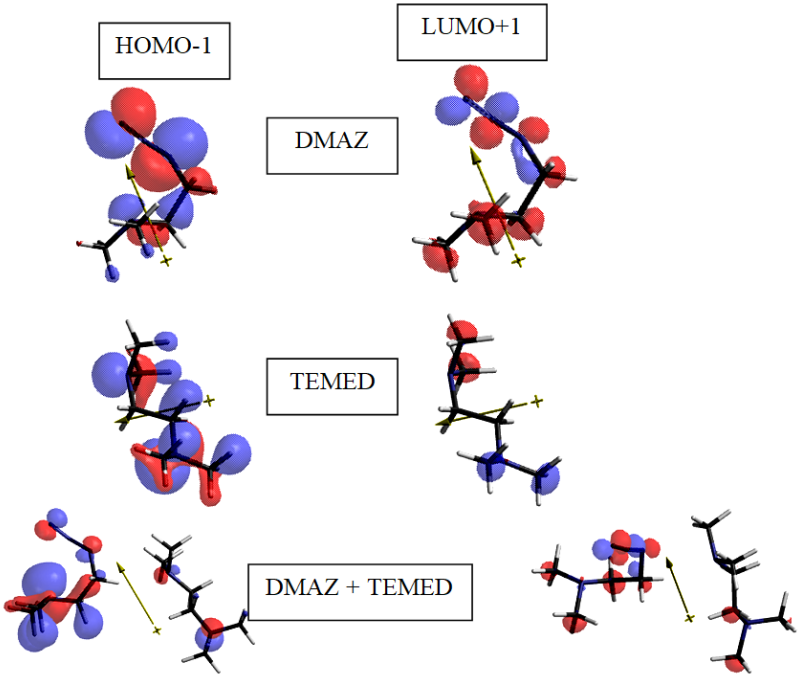

Figure 9. The HOMO-1 and LUMO+1 patterns.

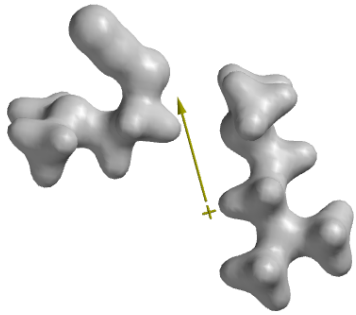

Figure 10. Bond density of the composite.

Chemical reactions quite often involve some charge transfer between recanting molecules (or between two different parts of the same molecule). The active sites of a reactant molecule are usually places where the addition or loss of electron(s) is/are favorable. So the understanding of chemical reactivity could be achieved by finding the best site where to add or remove an electron to a molecule is possible. The local ionization and the LUMO maps may give an idea for that purpose [35].

Figure 11 displays the local ionization and the LUMO maps of the composite system considered. In the local ionization potential map, conventionally red/reddish regions (if any exists) on the density surface indicate areas from which electron removal is relatively easy, meaning that they are subject to electrophilic attack. On the other hand, LUMO map displays the absolute value of the LUMO on the electron density surface. The blue color stands for the maximum value of the LUMO and the color red, the minimum value.

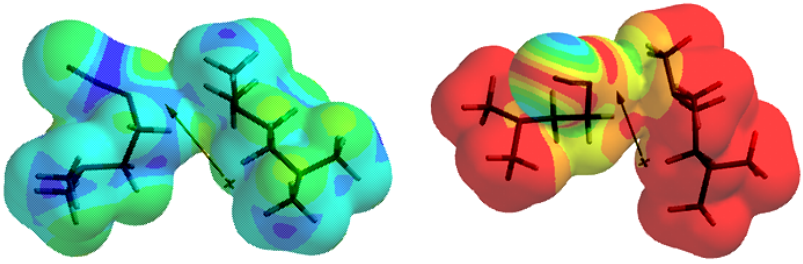

Figure 11. The local ionization (left) and the LUMO (right) maps of the composite system considered.

The over all analysis reveal that the interaction between DMAZ and TEMED is mainly electrostatic in nature and most probably arising from charge-charge, charge-dipole and dipole-dipole interactions which affect the potential field around the components. Some minor contributions coming to the frontier or the next frontier orbitals

from the partner of the major contributor indicates some orbital interactions as well. They might arise secondary orbital interactions which do not lead to any bond formations. However, under suitable conditions they might initiate some channels to initiate reactions between the components.

Actually, the ignition of a combustible mixture depends on various complex interactions between many physical and chemical processes. The over all competing rates of each process combine and dictate a global ignition delay time. The global ignition delay is typically grouped into a physical delay and a chemical delay [36]. The chemical delay is mainly determined by the activation energy characteristic of a given propellant admixture. Note that for gaseous propellants, the physical delay originates from the time necessary for heating, diffusion, and mixing. The physical delay in the case of liquid propellants, is lengthened by atomization and evaporation processes. It is greatly influenced by the injection technique employed and the physical properties of the propellants that control mixing, viscosity, surface tension, and miscibility of components.

4. Conclusion

The present study could be considered as a static picture of the interaction between the components in the absence of any hypergolic reaction. The global ignition delay which governs the start of hypergolic reaction depends of various factors. DMAZ end TEMED in vacuum conditions and the restrictions of the theory and the basis set employed interact with each other mainly electrostatically keeping their electronic integrity. However, some contributions to molecular orbitals of each other occurs which might trigger formations of hot points necessary for a hypergolic reaction if suitable conditions arise. They might be physical, chemical or catalytic in nature. Note that presently 1:1 composite of the components have been considered. Varying the composition might cause changing of the interaction profile thus leads to a hypergolic reaction.

References

[1] Jyoti, B.V.S., Naseem, M.S., & Baek, S.W. (2017). Hypergolicity and ignition delay study of pure and energized ethanol gel fuel with hydrogen peroxide. *Combustion and Flame*, *176*, 318-325. https://doi.org/10.1016/j.combustflame.2016.11.018

[2] da Silva, G., & Iha, K. (2012). Hypergolic systems: A review in patents. *J. Aerosp. Technol. Manag., São José dos Campos*, *4*(4), 407-412. https://doi.org/10.5028/jatm.2012.04043812

[3] U.S. Patent Number: 7,954,754 (2011). Hypergolic liquid or gel fuel mixtures, Application number: 12,131,248, Date of Patent: 7 Jun (2011). U.S. Army combat capabilities development command aviation & missile center.

[4] Di Salvo, R. (2012). High energy, low temperature gelled bi-propellant formulation preparation method. U.S. Patents 2012/0073713 A1.

[5] Hawkins, T.W., Schneider, S., Drake, G.W., Vaghjiani, G., & Chambreau, S. (2011). Hypergolic fuels. U.S. Patents 8,034,202 B1.

[6] Koppes, W.M., Rosenberg, D.M., Clark, K.A., Schlegel, E.S., Vos, B.W., Lang, J.W., & Warren, A.D. (2010). Reagents for hypergolic ignition of nitroarenes. U.S. Patents 7,648,602 B1.

[7] Natan, B., Valeriano, P., & Yair, S. (2011). Hypergolic ignition system for gelled rocket propellant. *World Intellectual Property Organization*, WO2011/001435 A1.

[8] Sengupta, D. (2008). High performance, low toxicity hypergolic fuel. U.S. Patents 2008/0202655 A1.

[9] Smith, J.R., Ogden, G.E., Brown, C.J., Frisby, P.M., & Torabzadeh, S.A. (2010). Hydroxyethylhydrazinium nitrate-acetone formulations and methods of making hydroxyethylhydrazinium nitrate-acetone formulations. U.S. Patents 2010/0287824 A1.

[10] Watkins, W.B., (2004). Hypergolic fuel system. U.S. Patents US2004/0177604 A1.

[11] Lauck, F., Negri, M., Freudenmann, D., & Schlechtriem, S. (2019). Study on hypergolic ignition of ionic liquid solutions. 8th European Conference for Aeronautics and Space Sciences (EUCASS), 1-10. https://doi.org/10.13009/EUCASS2019-653

[12] Melof, B., Grube, M., Sun, C., Tang, S., & Zhang, X. (2017). Role of cation structures for energetic performance of hypergolic ionic liquids. *Energy & Fuels*, *31*, 10055-10059. https://doi.org/10.1021/acs.energyfuels.7b01259

[13] Kang, H., & Kwon, S. (2017). Green hypergolic combination: Diethylenetriamine-based fuel and hydrogen peroxide. *Acta Astronautica*, *137,* 25-30. https://doi.org/10.1016/j.actaastro.2017.04.009

[14] Schneider, S., Hawkins, T., Ahmed, Y., Rosander, M., Mills, J., & Hudgens, L. (2011). Green hypergolic bipropellants: H_2O_2 / hydrogen-rich ionic liquids. *Agnewande Chemie International Edition*, *50*, 5886-5888. https://doi.org/10.1002/ange.201101752

[15] Kan, B. , Heister, S., & Paxson, D. (2017). Experimental study of pressure gain combustion with hypergolic rocket propellants. *Journal of Propulsion and Power*, *33*, 112-120. https://doi.org/10.2514/1.B36195

[16] Kurilov, M., Kirchberger, C., Freudenmann, D., Siefel, A., & Ciezki, H. (2018). A method for screening and identification of green hypergolic bipropellants. *International Journal of Energetic Materials and Chemical Propulsion*, *17*(3), 183-203. https://doi.org/10.1615/intjenergeticmaterialschemprop.2018028057

[17] Kim, Y.-S., Son, G.-H., Na, T.-K., & Choi, S.-H. (2015). Synthesis and physical and chemical properties of hypergolic chemicals such as N,N,N-trimethylhydrazinium and 1-ethyl-4-methyl-1,2,4-triazolium salts. *Applied Sciences*, *5*(4), 1547-1559. https://doi.org/10.3390/app5041547

[18] Chinnam, A., Petrutik, N., Wang, K., Shlomovich, A., Shamis, O., Toy, D., Suceska, M., Yan, Q.-L., Dobrovetsky, R., & Gozin, M. *(*2018). Effects of *closo*-icosahedral periodoborane salts on hypergolic reactions of 70% H_2O_2 with energetic ionic liquids. *Journal of Materials Chemistry A*, *6*, 19989-19997. https://doi.org/10.1039/C8TA03780A

[19] Daimon, W., Gotoh, Y., & Kimura, I. (2012). Mechanism of explosion induced by contact of hypergolic liquids, *J. Propulsion*, *7*(6), 946-952. https://doi.org/10.2514/3.51323

[20] Pourpoint, T.L., & Anderson, W.E. (2007). Hypergolic reaction mechanisms of catalytically promoted fuels with rocket grade hydrogen peroxide, *Combustion Science and Technology*, *10*, 2107-2133. https://doi.org/10.1080/00102200701386149

[21] Stewart, J.J.P. (1989). Optimization of parameters for semi empirical methods I. *J. Comput. Chem*., *10*, 209-220. https://doi.org/10.1002/jcc.540100208

[22] Stewart, J.J.P. (1989). Optimization of parameters for semi empirical methods II. *J. Comput. Chem*., *10*, 221-264. https://doi.org/10.1002/jcc.540100209

[23] Leach, A.R. (1997). *Molecular modeling*. Essex: Longman.

[24] Kohn, W., & Sham, L.J. (1965). Self-consistent equations including exchange and correlation effects. *Phys. Rev*., *140*, 1133-1138. https://doi.org/10.1103/PhysRev.140.A1133

[25] Parr, R.G., & Yang, W. (1989). *Density functional theory of atoms and molecules*. London: Oxford University Press.

[26] Becke, A.D. (1988). Density-functional exchange-energy approximation with correct asymptotic behavior. *Phys. Rev. A*, *38*, 3098-3100. https://doi.org/10.1103/PhysRevA.38.3098

[27] Vosko, S.H., Wilk, L., & Nusair, M. (1980). Accurate spin-dependent electron liquid correlation energies for local spin density calculations: a critical analysis. *Can. J. Phys*., *58*, 1200-1211. https://doi.org/10.1139/p80-159

[28] Lee, C., Yang, W., & Parr, R.G. (1988). Development of the Colle-Salvetti correlation energy formula into a functional of the electron density. *Phys. Rev. B*, *37*, 785-789. https://doi.org/10.1103/PhysRevB. 37.785

[29] Cramer, C.J. (2004). *Essentials of computational chemistry*. Chichester, West Sussex: Wiley.

[30] SPARTAN 06 (2006). Wavefunction Inc. Irvine CA, USA.

[31] Pakdehi, S.G., Rezaei, S., Motamedoshariati, H., & Keshavarz, M.H. (2014). Sensitivity of dimethyl amino ethyl azide (DMAZ) as a non-carcinogenic and high performance fuel to some external stimuli. *Journal of Loss Prevention in the Process Industries*, *29*, 277-282. https://doi.org/10.1016/j.jlp.2014.03.006

[32] Türker, L. (2011). Recent developments in the theory of explosive materials. In J. Thomas (Ed.). *Explosive materials* (pp. 1-52). New York: NOVA Pub.

[33] Barrow, G.M. (1962). *Introduction to molecular spectroscopy*. Tokyo: McGraw-Hill (Int. Student Ed.).

[34] Harris, D.C., & Bertolucci, M.D. (1978). *Symmetry and spectroscopy: an introduction to vibrational and electronic spectroscopy*. New York: Oxford University Press.

[35] Ayers, P.W., & Parr, R.G. (2000). Variational principles for describing chemical reactions: The Fukui function and chemical hardness revisited, *J. Am. Chem. Soc*., *122*, 2010-2018. https://doi.org/10.1021/ja9924039

[36] Hampton, C.S., Ramesh, K.K., & Smith, J.E. (2003). Importance of chemical delay time in understanding hypergolic ignition behaviors. AIAA-2003-1359. *41st Aerospace Sciences Meeting and Exhibit*. https://doi.org/10.2514/6.2003-1359